

Supporting Information

Wide-Bandgap Organic Nanocrystals with High Mobility and Tunable Lasing Emission

Yin-Xiang Li,^a Wei Liu,^b Meng-Na Yu,^c Xue-Mei Dong,^a Chang-Jin Ou,^a Mustafa Eginligil,^a
Rui-Qing Li,^c Xin-Wen Zhang,^c Yi-Jie Nie,^a Ling-Hai Xie,^c Chun-Xiang Xu,^b Ju-Qing Liu,^{a,*}
Wei Huang^{a,d,*}

^aKey Laboratory of Flexible Electronics (KLOFE) & Institute of Advanced Materials (IAM), Jiangsu National Synergetic Innovation Center for Advanced Materials (SICAM), Nanjing Tech University (NanjingTech), 30 South Puzhu Road, Nanjing 211816, China.

^bState Key Laboratory of Bioelectronics, School of Biological Sciences & Medical Engineering, Southeast University, Nanjing 210096, China.

^cCentre for Molecular Systems and Organic Devices (CMSOD), Key Laboratory for Organic Electronics and Information Displays & Institute of Advanced Materials (IAM), Jiangsu National Synergetic Innovation Center for Advanced Materials (SICAM), Nanjing University of Posts & Telecommunications, 9 Wenyuan Road, Nanjing 210023, China.

^dFrontiers Science Center for Flexible Electronics, Xi'an Institute of Flexible Electronics (IFE) and Xi'an Institute of Biomedical Materials & Engineering, Northwestern Polytechnical University, 127 West Youyi Road, Xi'an 710072, China.

Experimental Section

Materials: All solvents were purchased from Aldrich or J&K Chemicals without further purification. BMeF was synthesized by a simple one-step Suzuki reaction according to our previous report.^[1]

The preparation of BMeF macroscopic crystal and nanocrystals: Macroscopic single crystals of BMeF were obtained from the saturated tetrahydrofuran: isopropanol = 1:5 at room temperature. After aged two weeks, single crystal suiting for X-ray diffraction was obtained. The crystallographic data of BMeF are given in Table S3. 2D hexagon disks were prepared by a facile antisolvent vapor-assisted crystallization (AVC) strategy. Figure S2 displays the working setup of the two-vial-based AVC. Typically, the inner vial contains the solution of BMeF in tetrahydrofuran (THF) with varying concentrations (C_{BMeF}) and the outer vial contains methanol as the antisolvent. Slow diffusion of the methanol vapor from the outer vial into the inner vial at room temperature gradually obtains crystalline structures. Elongated hexagon microdisks (EHDs) with the edge length (a) of 27.5 μm were obtained at $C_{\text{BMeF}} = 1 \text{ mM}$. EHDs with edge length of 67.3 μm were obtained at $C_{\text{BMeF}} = 10 \text{ mM}$. EHDs with the edge length (a) of 13.2 μm were obtained at $C_{\text{BMeF}} = 0.2 \text{ mM}$. In general, the edge length (a) of the BMeF EHDs is proportion to the C_{BMeF} of the BMeF in THF.

Characterization: Absorption spectra were measured with a Shimadzu UV-3600 spectrometer at 25°C, and emission spectra were recorded on a Shimadzu RF-5301(PC) luminescence spectrometer. The absolute photoluminescence quantum efficiency of spin-coating film and crystal of BMeF was measured by Edinburgh Instruments FLS-920 in integrating sphere. The experimental parameters of fluorescence lifetime measurements are show as follows. The incident 390-nm, 150-fs laser pulses were generated from a Coherent TOPAS-C optical parametric amplifier; pumped by a 1 kHz Coherent Legend regenerative amplifier that is seeded by a Coherent Vitesse oscillator. These input laser pulses were focused by a lens ($f = 20 \text{ cm}$) on the sample solutions in a 1-mm-thick quartz cell (beam spot $\sim 1 \text{ mm}$ inside the cell). The emission from the samples was collected at a back scattering angle of 150° by a pair of lenses and directed to an Optronis Optoscope™ streak camera system which has an ultimate temporal resolution of 6 ps. The transmission electron microscopy (TEM) and selected-area electron diffraction (SAED) studies were performed in a JEM 2010F JEOL, operating at an accelerating voltage of 100 kV. The powder X-ray diffraction (XRD) patterns were performed on a Bruker D8 X-ray diffractometer with Cu K α radiation ($\lambda = 1.54050 \text{ \AA}$). The operating 2θ angle ranges from 5 to 30 \AA , with the step length of 0.025°. The electronic structure calculation for the BMeF is carried out with time-dependent density functional theory (TD-DFT) in Gaussian quantum chemistry package. 6-31G (d) basis set and B3LYP functional are applied to all calculations.

The characterization of microcrystal lasers: The excitation source is a liquid-nitrogen-cooled laser (COHERENT Libra-F-HE) with 325 nm femtosecond pulse laser at a repetition of 1000 Hz and pulse duration of 150 fs. The lasing spectra of the microcrystals were excited by a focused 325 nm laser through a confocal μ -PL system (OLYMPUS BX53). The size of light spot was about 20 μm in diameter. The luminescent

light was collected through an optical multichannel analyzer (Princeton, Acton SP2500i) and the spectral resolution of the spectrometer is 0.167 nm. All measurements were performed at ambient atmosphere. The pump fluence (P) = $(P_0/f)/A$, where P_0 is pump power, which is measured via power meter, f is the repetition frequency, and A is light spot area.

OFET and OLED device fabrications and measurements: Single crystals for OFETs were prepared by the above AVC strategy. The crystals were directly growth on the OTS-modified Si/SiO₂ substrate. The bottom-gate, top-contact device configuration was fabricated by a “glue the gold film” technique, then, the OFET characteristics were recorded by a Keithley 4200 SCS and Summit 11000B-M probe station. Vertical light-emitting diodes (OLEDs) based on BMeF have the following structure: ITO/ 40nm NPB/20 nm BMeF/30 nm TMPYPB/1 nm LiF/Al. The EL spectra and CIE coordinates of the devices were recorded by a spectra-scan PR655 spectrophotometer. The emission area of the devices is 9 mm². The current-voltage luminescence characteristics were measured using a combination of a Keithley source meter (model 2602) and a luminance meter. All the devices were characterized without encapsulation, and all the measurements were carried out in the ambient condition at room temperature (RT).

[CCDC 1997206 contains the supplementary crystallographic data for this paper. These data can be obtained free of charge from The Cambridge Crystallographic Data Centre via www.ccdc.cam.ac.uk/data_request/cif.]

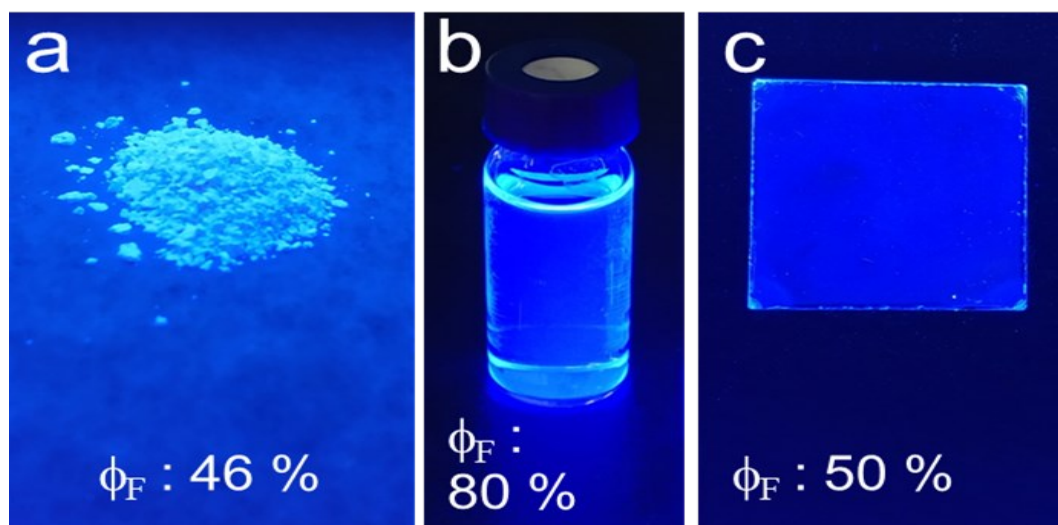


Figure S1. The fluorescence photographs of (a) BMeF powder, (b) BMeF solution in THF and (c) BMeF spin-coated film, under illumination of a handheld UV (365 nm) lamp, respectively.

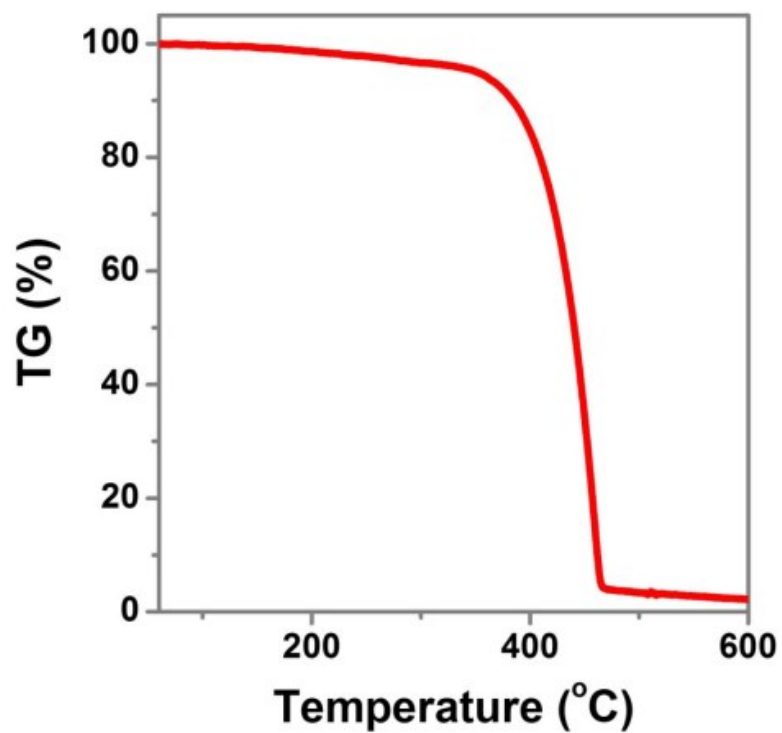


Figure S2. TGA curve of BMeF

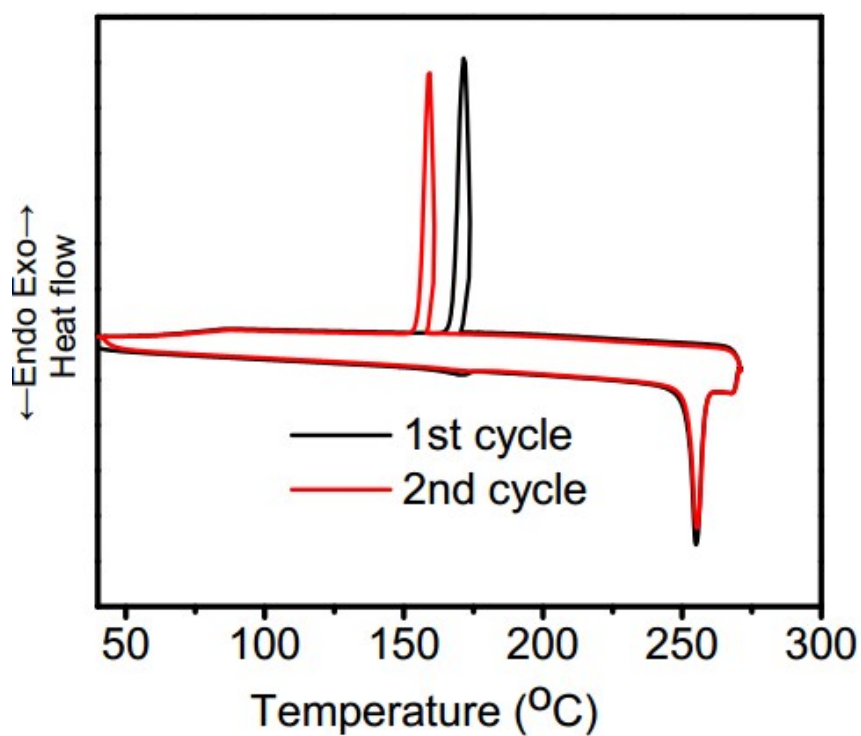


Figure S3. DSC curves of BMeF

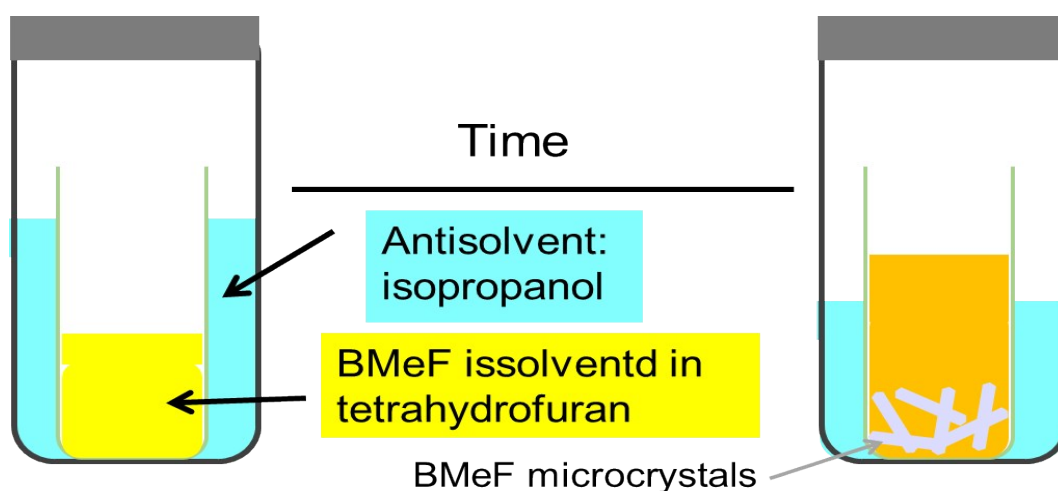


Figure S4. Schematic diagram of the AVC process for BMeF microcrystals.

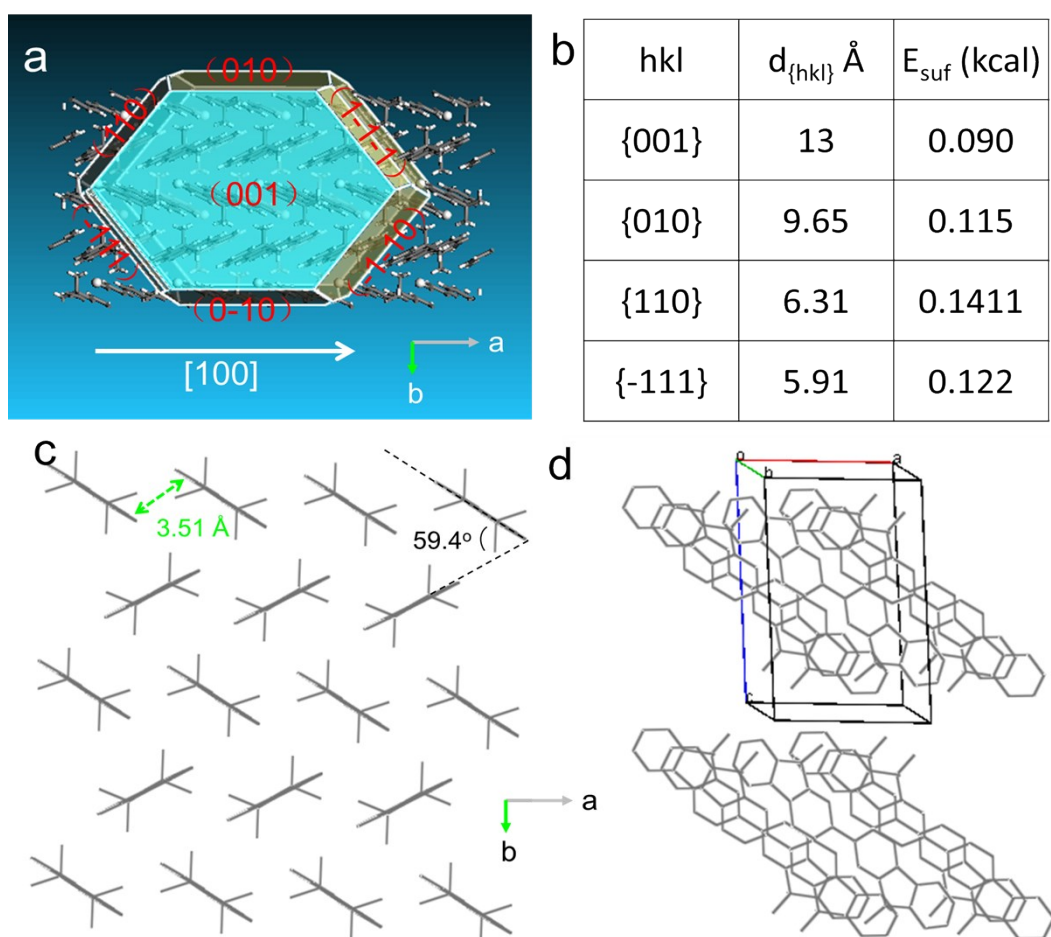


Figure S5. (a) Theoretically predicted growth morphology of a BMeF crystal based on the attachment energies calculated with Materials Studio package. (b) Molecular packing of the BMeF single crystal.

From the simulation results in Figure S3a, we found that the thermodynamically stable morphology for compound BMeF is a well-defined 2D hexagon-like

morphology. The calculated surface energies (hkl) of the various crystal faces (hkl) are displayed in Figure S3b, and the lowest surface free energy of $\{001\}$ revealing it is the most thermodynamically stable surface. Furthermore, the $\{1kl\}$ s face with the highest surface energy implies the hexagon can preferentially grow along the direction because the kinetic barrier of growth for (hkl) is inversely proportional to the surface energy of (hkl). The BMeF molecules are arranged in slip-stacks along the short molecular axis with the π - π stacking distance of 3.51 Å (Figure S3c). The long axis of the molecule is tilted by 45° with respect to the crystallographic c -axis (Figure S3d). No hydrogen bond or other interactions exist between two adjacent molecules, and the π - π interaction might be the dominating driving force which facilitates the BMeF crystal growth along the $[1kl]$ direction forming a long or elongated 2D hexagon disk.

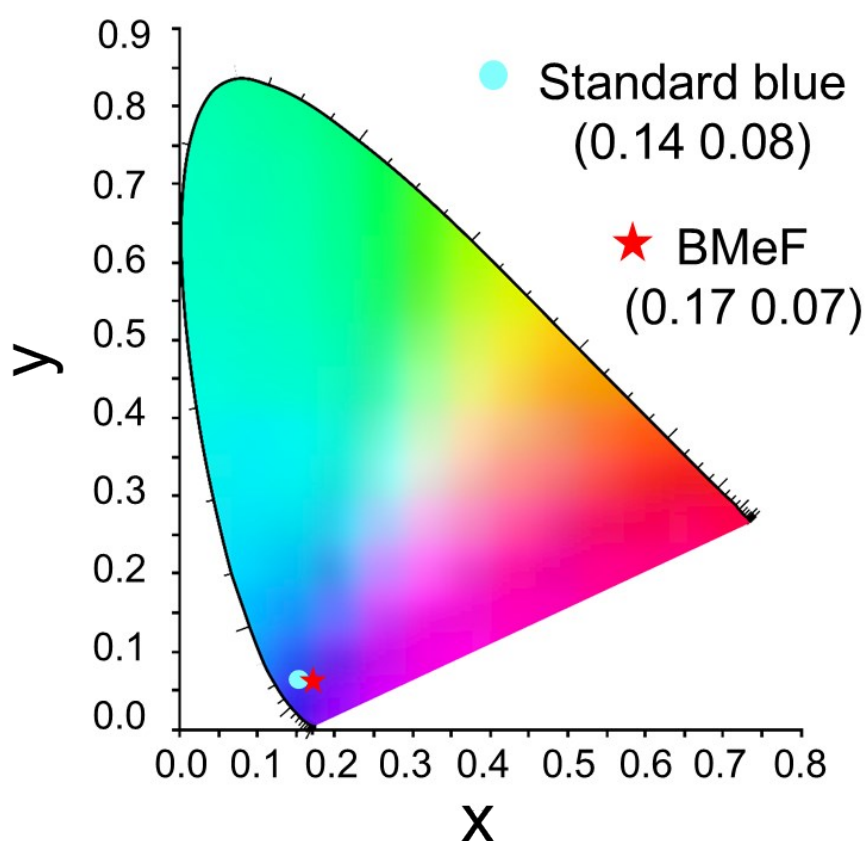


Figure S6. CIE 1931 coordinates of the BMeF solution.

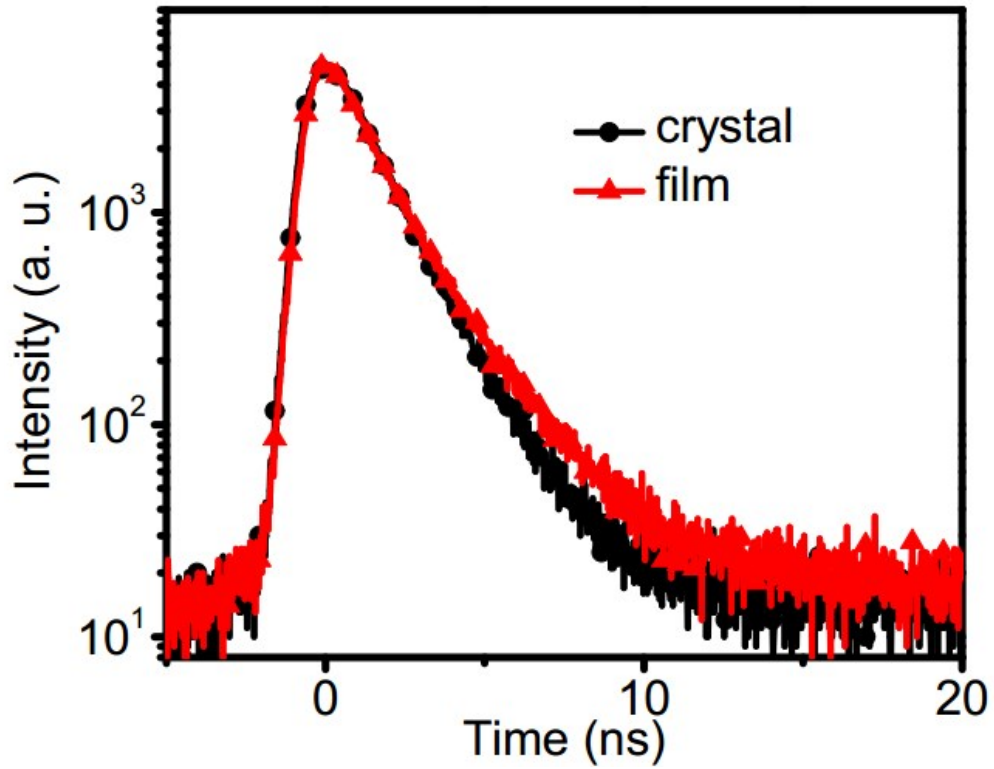


Figure S7. Life decay-time of BMeF crystal and spin-coated films.

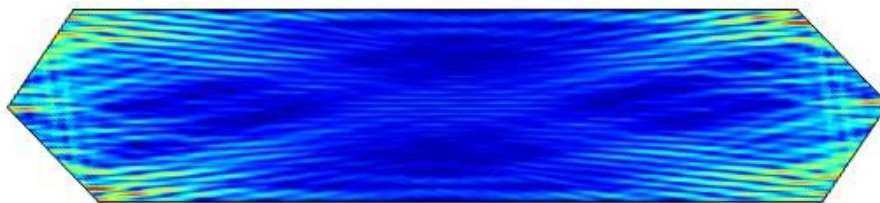


Figure S8. Simulated field intensity distribution ($\lambda = 392$ nm, $n = 1.52$) in the BMeF microdisk with edge length (a) of $18.6 \mu\text{m}$.

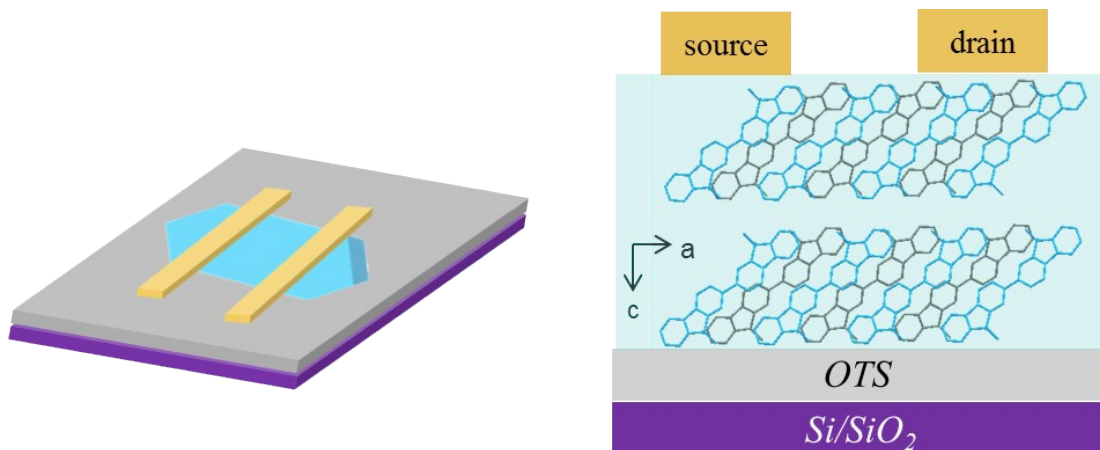


Figure S9. Schematic of BMeF based transistor with bottom-gate top-contact device geometry.

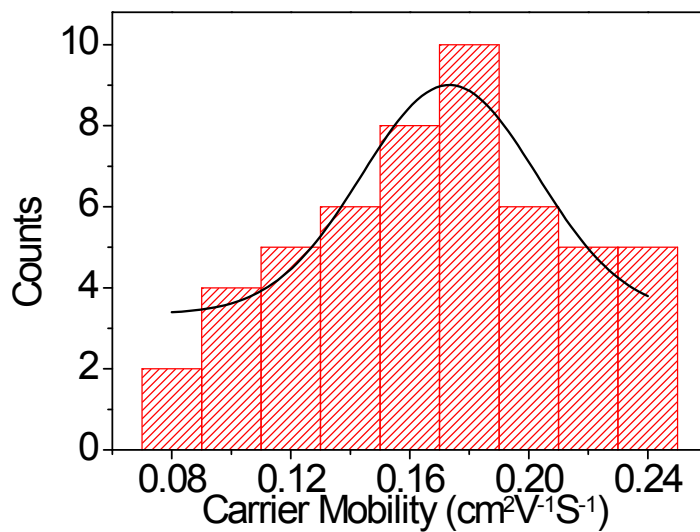


Figure S10. Mobility histogram of BMeF crystal-based OFETs

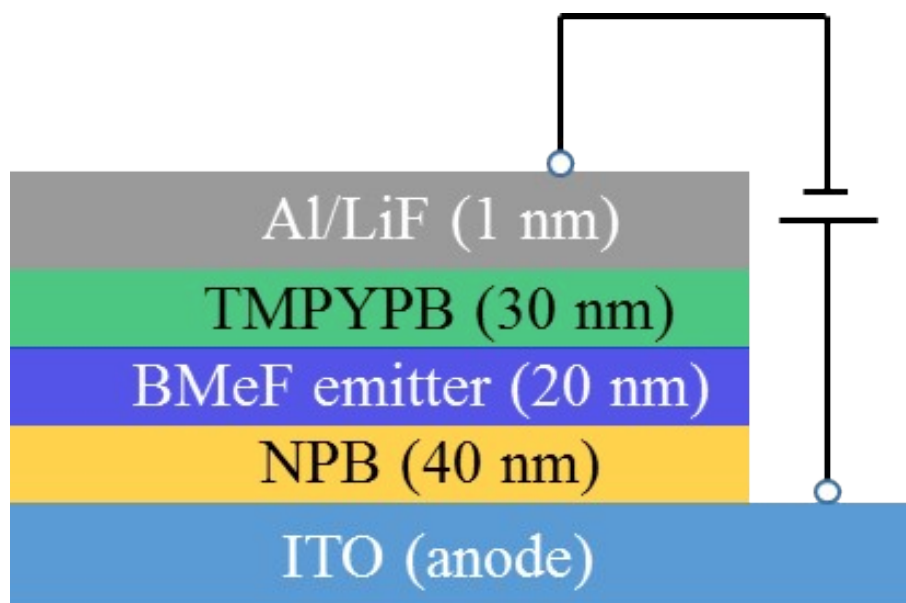


Figure S11. OLEDs based on BMeF with NPB, LiF and TMPYPB as buffer layers.

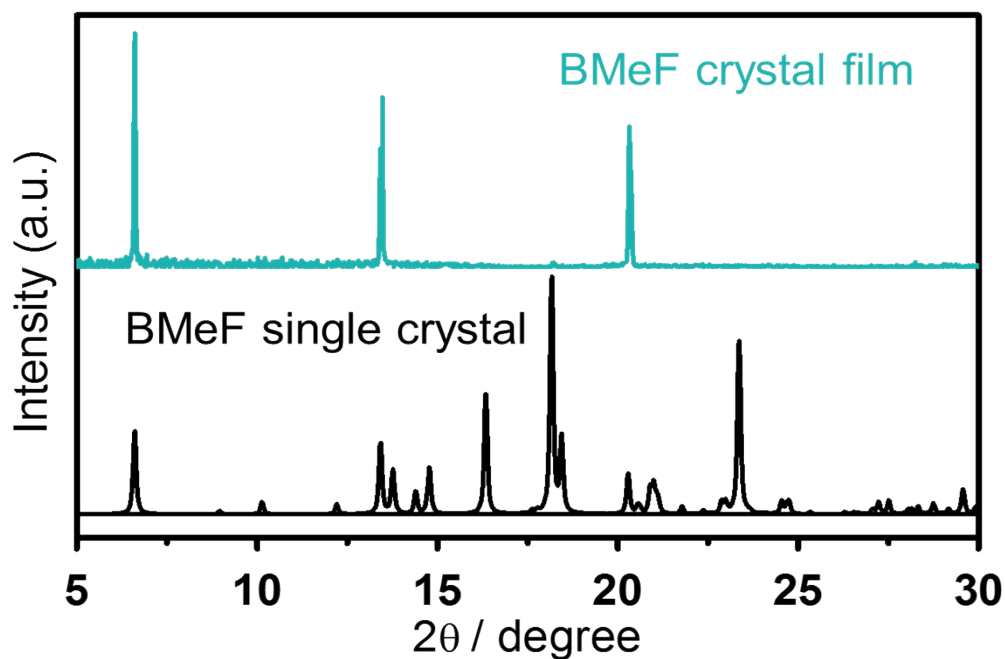
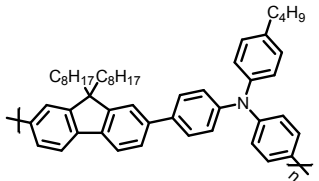
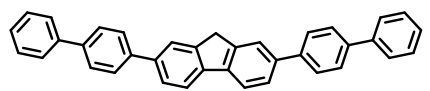
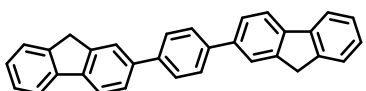
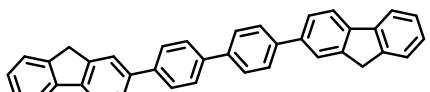
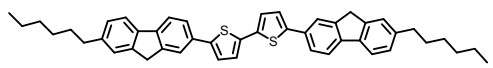
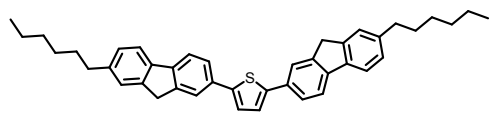
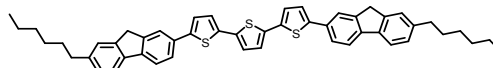
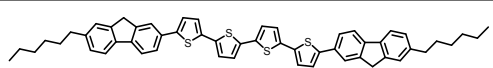
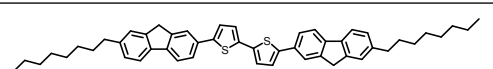
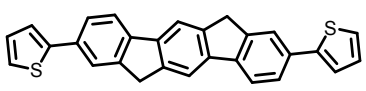
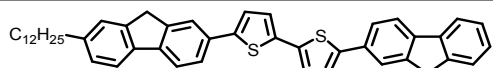
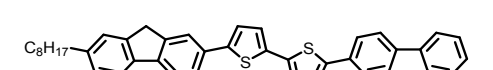
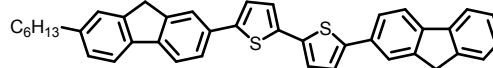
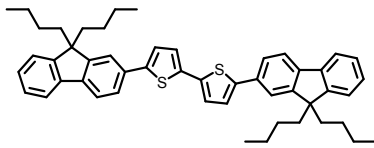
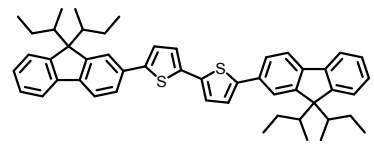
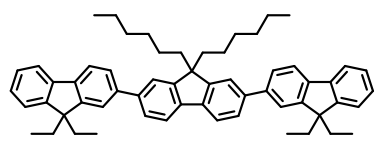
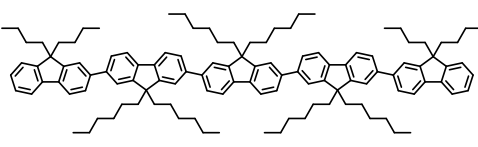
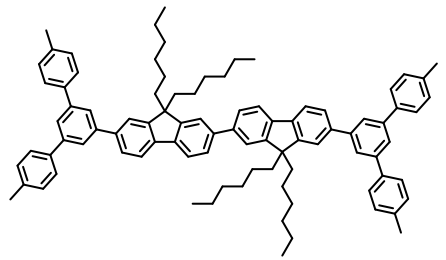


Figure S12. XRD patterns of the as-prepared BMeF emitter layer (top) and the standard powder spectrum based on the single crystal data by using the DIAMOND software (bottom).

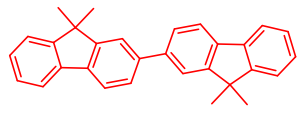
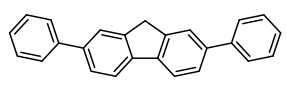
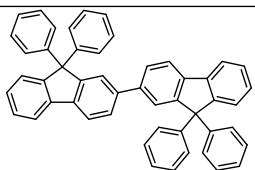
Table S1. A summary of organic field-effect transistor performances based on fluorene derivatives till now reported in literatures.

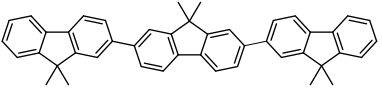
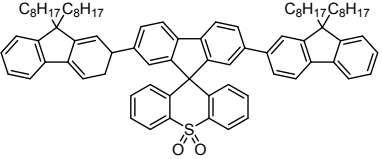
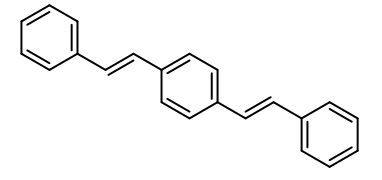
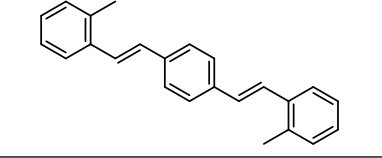
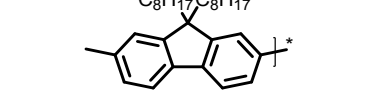
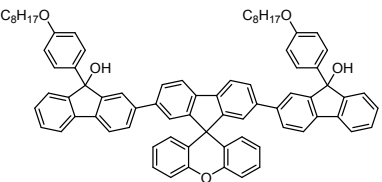
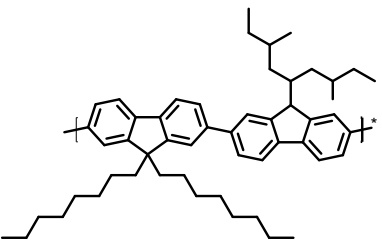
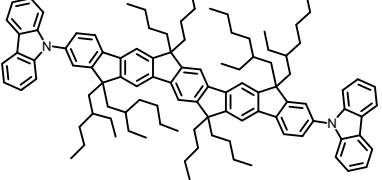
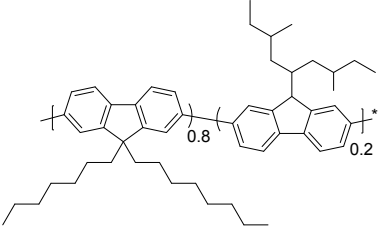
Materials	Mobility [$\text{cm}^2 \text{V}^{-1} \text{s}^{-1}$]	VT [V]	$I_{\text{on/off}}$	Reference
	0.25 (sc)	6	10^6	<i>J. Am. Chem. Soc.</i> 2020 , 142, 6332-6339.
	0.11 (sc)	/	/	<i>J. Am. Chem. Soc.</i> 2001 , 123, 9214-9215
	0.08 (sc)	/	/	
	0.06	-24	10^4	<i>Chem. Mater.</i> 2005 , 17, 3861-3870
	10^{-5}	18	10^3	<i>Thin Solid Films</i> 2007 , 515, 7318-7323
	10^{-3}	45	10^4	

	10 ⁻³	-50	10 ³	<i>Appl. Phys. Lett.</i> 2005 , 87, 3.	
	0.06	/	10 ⁶	<i>Adv. Mater.</i> 2006 , 18, 2989-2992.	
	0.014	/	10 ⁶	<i>Chem. Mater.</i> 2003 , 15, 1778-1787	
	0.32	/	10 ⁷		
	0.14 (180 °C)	/	10 ⁴		
	0.012 (180 °C)	/	10 ³		
	0.025 (180 °C)	/	10 ²		
	0.023 (180 °C)	/	10 ²		
	0.184 (90 °C)	/	/		<i>Chem. Mater.</i> 2007 , 19, 5882-5889
	0.012	-55	/		<i>J. Vac. Sci. Technol. A</i> 2006, 24, 654-656.
	0.15 ± 0.009 (140 °C)	-7	10 ⁶		<i>Chem. Mater.</i> 2006 , 18, 6250-6257
	0.10 ± 0.001 (140 °C)	-8	10 ⁶		
	0.097 ± 0.0004 (140 °C)	-4	10 ⁶		

	3×10^{-4}	/	10^4	<i>Chem. Mater.</i> 2006 , <i>18</i> , 2311-2317
	10^{-5}	/	10^4	
	9×10^{-3}	/	/	<i>Dyes and Pigments</i> 2015 , <i>123</i> , 370-379
	3.8×10^{-5}	-36	10^4	<i>Phys. Chem. Chem. Phys.</i> 2014 , <i>16</i> , 16941-16956
	3×10^{-4}	/	/	<i>Chem. Commun.</i> 2016 , <i>52</i> , 3103-3106

Tbale S2. A summary of organic lasing materials that integrate shortwave (< 450 nm) laser and charge carrier transport laser property.

Materials	λ (nm)	Laser P_{th}	PLQY	Mobility [$\text{cm}^2 \text{V}^{-1} \text{s}^{-1}$]	Reference
	392 415	$2.77 \mu\text{J cm}^{-2}$ $3.80 \mu\text{J cm}^{-2}$	75 %	0.18	This work
	407	$30 \mu\text{J cm}^{-2}$	60 %	0.25	<i>J. Am. Chem. Soc.</i> 2020 , <i>142</i> , 13, 6332–6339
	402	46.5 W cm^{-2}	54 %	/	<i>J. Mater. Chem. C</i> , 2017 , <i>5</i> , 5345-5355

	412	114 W cm ⁻²	53 %	/	<i>J. Phys. Chem. C</i> , 2017 , 121, 14803-14810
	407	41.5 W cm ⁻²	58 %±2 %	/	<i>Mater. Chem. Front.</i> , 2018 , 2, 2307-2312
	440	790 nJ cm ⁻² (a)	65 %	/	<i>Angew. Chem. Int. Ed.</i> 2014 , 53, 1-6
	448	14 μJ cm ⁻² (a)	90 %	/	<i>J. Am. Chem. Soc.</i> , 2014 , 136, 16602-16608
	445	1.5 μJ cm ⁻² (b)	50±5 %	2.66×10 ⁻⁴	<i>Adv. Optic. Mater.</i> , 2017 , 5, 1700123
	447	56 kW cm ⁻²	65 % (crystal)	/	<i>Chem</i> 2019 , 5, 2470-2483.
	448	0.5 μJ/cm ²	70±5% (film)	3.7×10 ⁻²	<i>Nat. Mater.</i> 2008 , 7, 376-380
	447	0.6 nJ/pulse ⁻¹	25±5 %	1×10 ⁻³	<i>Adv. Opt. Mater.</i> 2017 , 5, 160100.
	451	0.3 μJ/cm ²	60±5 %	2.67×10 ⁻²	

(a) pulse width and frequency: 150 fs, 1 kHz; (b) pulse width and frequency: 300 fs, 1 kHz.

Table S3. Crystal Data and Structure Refinement for BMeF (CCDC: 1997206).

Parameters	BMeF crystal
Empirical formula	C ₃₀ H ₂₆
Formula weight	386.51
Temperature	293.15 K
Wavelength	0.71073 Å
Crystal system	triclinic
Space group	P-1
Unit cell dimensions	a = 8.390(3) Å, α = 79.129(11)
	b = 9.828(3) Å, β = 87.424(7)
	c = 13.251(4) Å, γ = 89.762(7)
Z	2
Density (calculated)	1.179 g cm ⁻³
Absorption coefficient	0.067 mm ⁻¹
F(000)	412

Author Contributions

Yin-Xiang Li, Ju-Qing Liu and Wei Huang performed the major study and wrote the manuscript. Yin-Xiang Li and Chang-Jing Ou were responsible for the preparation and structure characterization. Yin-Xiang Li, Wei Liu, Xue-Mei Dong and Chun-Xiang Xu collected the lasing data. Yin-Xiang Li, Chang-Jin Ou and Yi-Jie Nie obtained the single crystal and analysed the data. Yin-Xiang Li, Wei Liu and Xue-Mei Dong fabricated the OFETs. Yin-Xiang Li, Meng-Na Yu, Rui-Qing Li and Xin-Wen Zhang carried out the OLED experimental sections. Meng-Na Yu and Xue-Mei Dong did SEM and optical microscope analysis. Ju-Qing Liu and Mustafa Eginligil revised the manuscript and provided some suggestions. All authors discussed the results and commented on the manuscript at all stages.

1. W. S. Zhu, Y. M. Han, X. An, J. N. Weng, M. N. Yu, L. B. Bai, C. X. Wei, J. Y. Lin, W. Liu, C. J. Ou, L. H. Xie, X. H. Ding, J. F. Zhao, C. X. Xu, W. J. Huang, *J. Phys. Chem. C*, **2019**, *123*, 28881.